Computer Assisted Mechanics and Engineering Sciences, 10: 201–210, 2003.

Incomplete sensitivities in design and control of fluidic channels[†]

Bijan Mohammadi
Montpellier University, Math. Dept., 34090 Montpellier, France

Juan Santiago
Stanford University, Mechanical Engineering Dept., CA 94305-3032, USA

(Received October 25, 2002)

We would like to show how to perform shape optimization and state control at a cost comparable to the one of analysis. To this end, we propose to only use informations available for cost function evaluation and incomplete sensitivities not requiring the solution of the linearized state equation. The application of the method is presented for microfluidic MEMs design and control.

1. Introduction

Control of distributed systems has various possible industrial applications as we are often interested in keeping complex multi-disciplinary systems in some given states. Control space definition or parameterization is the first main issue we face when targeting to formulate a control problem. Usually, one wishes to keep the parameterization space dimension as low as possible and hence limit the complexity of the problem. In addition, for any control approach to be efficient, it has to be realizable during the time the system is still controllable. Computational cost is therefore another essential issue. Our aim through the paper is to discuss alternatives to these two difficulties.

Our aim through this paper is to discuss the behavior of our design and control platform on two complementary situations: where the number of control is small (basically one) and where the number of control is large. We present our sub-optimal control technique using accurate gradient evaluation for the first class of problem and for the second class of applications, we show that the sub-optimal control is also efficient using incomplete evaluation of the gradient, but this only for some class of cost functions. Our motivation here comes from the fact that for a control algorithm based on gradient methods to be efficient, we need the design to have the same complexity than the direct problem. We need therefore a cheap and easy gradient evaluation somehow avoiding the adjoint equation solution.

The problem being multi-disciplinary, we need to couple different state equations during control. In that context, the gradient-based minimization algorithm is reformulated as a dynamic system as is considered as an extra state equation for the parameterization. This formulation makes easier to understand the coupling between the different ingredients. Hence, we look for the solutions of our optimization problem as stationary solutions of a second order dynamic system. In addition, for the system to have global search features, we use the natural instability of second order hyperbolic systems [1].

[†]This is an extended version of a paper presented at the conference *OPTY-2001, Mathematical and Engineering Aspects of Optimal Design of Materials and Structures*, Poznań, Poland, August 27–29, 2001.

2. Dynamic shape optimization and state control

Consider the following optimization or control problem,

$$\min_{x(t)} J(x(t), q(x), U(q), \nabla U(q)), \tag{1}$$
$$E(x(t), q(x), U(q), \nabla U(q)) = 0, \qquad g_1(x(t)) \leq 0, \qquad g_2(q) \leq 0, \qquad g_3(q, U(q)) \leq 0,$$

where J is the cost function, $x \in R^n$ describes the parameterization q describes geometrical entities (normals, surfaces, volumes, ...). $U \in R^N$ denotes the state variables. $E \in R^N$ is the time dependent state equations. g_1 defines the constraints on the parameterization, g_2 those on geometrical quantities and g_3 state constraints. Details on the definition of the control and design configurations are given in [9].

2.1. State equations

The problem of interest here concerns separation of small suspended quantities in buffer solutions using their difference of mobility in an electric field.

The electric field $E = -\nabla\phi$ (V/m) is a solution of the following Poisson–Boltzmann equation for the potential ϕ (V),

$$\nabla \cdot E = -\Delta\phi = \frac{F}{\epsilon_r \epsilon_0}\rho_e \qquad \text{in } \Omega$$
$$\phi(\Gamma_{\text{in}}) = v_1\,, \qquad \phi(\Gamma_{\text{out}}) = v_2\,,$$
$$\phi = \phi_3 \quad \text{or} \quad \frac{\partial\phi}{\partial n} = 0 \qquad \text{on other boundaries.}$$

where $\rho_e = \sum_{i=1}^{n} z_i C_i$ is the net charge density (C/m^3), $z_i \in \mathbf{Z}$ is the valence number for specie i of molar concentration C_i (mol/m^3). F is the Faraday constant ($F = 96500$) and ϵ_r and ϵ_e are permitivity constants (resp. called relative and vacuum permitivities). The dielectric constant $F/(\epsilon_r\epsilon_0) \sim 10^{16}$. It is important to notice that for most applications, the net charge density is nearly zero.

The flow motion is described by the Navier–Stokes equations with Lorentz forces,

$$\rho\frac{\partial U}{\partial t} - \mu\Delta U + \nabla p = \rho_e \nabla\phi, \qquad \text{in the channel}$$
$$U = 0 \qquad \text{on walls}$$
$$-\mu\frac{\partial U}{\partial n} + p \cdot n = 0 \qquad \text{in and outflow boundaries.}$$

One difficulty in electro-osmotic flows is the computation of a sharp boundary around walls called the electric double layer (EDL) appearing due to the polarization of the walls. The boundary layer is only a few nanometer thick which implies a very fine mesh normal to the wall. We would like to avoid computing this area using the following more sophisticated boundary condition in place of the classical no-slip boundary condition above at the edge of the EDL,

$$U = \frac{-\epsilon_0\epsilon_r E\zeta}{\mu}\,, \tag{2}$$

where μ is the dynamical viscosity (kg/(ms)), ρ the flow density (kg/m^3), p the pressure (Pa) and U the flow velocity (m/s).

$\zeta(C_i)$ is called the zeta potential (V) and is a function of the local species concentration and characterizes the wall polarization due to external electric field and local ions.

The species are advected using the following advection-diffusion-reaction equations,

$$\frac{\partial C_i}{\partial t} = -\nabla \cdot j_i$$

where

$$j_i = -\nu_i z_i F C_i \nabla\phi - D_i \nabla C_i + C_i U + R_i(C),$$

and with ν_i being the mobility (mol·s/kg), D_i the diffusivity (m^2/s) and R_i the reaction term for specie i.

The net charge in the flow is find solving the following general Ohm law obtained after a summation of the species equations,

$$\frac{\partial \rho_e}{\partial t} = -\nabla \cdot i = 0,$$

with i the current charge density,

$$i = F \sum_{i=1}^{n} z_i j_i,$$

and j_i is the molar flux (s·mol/m^2) for specie i,

$$j_i = -\nu_i z_i F C_i \nabla\phi - D_i \nabla C_i + C_i U,$$

and with ν_i being the mobility (mol s/kg) and D_i the diffusivity (m^2/s) of specie i. This equation being conservative, its solution permits to correct any loss of conservation due to the solution.

For the particular case of electric neutral flows (i.e. $\rho_e = 0$), from equations above, we have a new equation for the potential ϕ instead of the Poisson–Boltzmann equation,

$$-F\nabla \cdot \left(\left(\sum_{i=1}^{n} \nu_i z_i C_i \right) \nabla\phi \right) = \nabla \cdot \left(\sum_{i=1}^{n} D_i z_i \nabla C_i \right).$$

This ensemble is therefore quite complex and it would be interesting not to use it for sensitivity evaluation. This is the motivation of using incomplete sensitivities presented below [8].

2.2. Closure equation for $x(t)$

In our approach minimization algorithms are seen as closure equation for the parameterization. In other words, we introduce a new time dependent problem for $x(t)$. This can also be seen as an equation for the structure. We can show that most linear or quadratic gradient based minimization algorithms can be put under the following form,

$$-\dot{x} + \epsilon \ddot{x} = F(\Pi, M^{-1}, (\nabla_{xx} J)^{-1}, \nabla_x J), \tag{3}$$

where F is a function of the exact or incomplete gradient and of the inverse of the Hessian of the cost function. It also takes into account the projection over the admissible space Π and the smoothing operator we use when using the CAD-free parameterization [5, 8]. Usually, Π does not depend on p except when using mesh adaptation.

Let us consider the particular case of $\epsilon > 0$, where we recover the so called heavy ball method [1–3, 7, 8]. The aim in this approach is to access different minima of the problem and not only the nearest local minimum by helping to escape from local minima after introduction of second order perturbation term. The difference with the original heavy ball method is based on the fact that here

the method is seen as a perturbation of the first order derivative while in the original heavy ball method the steepest descent is seen as a perturbation of the hyperbolic second order system. This reformulation is suitable for numerical experiences as it enables to tune the perturbation to be the weakest possible. Indeed, otherwise especially for complex applications, the optimization process becomes hard to control.

Another interesting feature of dynamic minimization algorithm is a possible coupling between several balls (point in the admissible control space) to improve the global search ability of the method by communicating informations between balls on their respective state. The idea is therefore to solve the pseudo-unsteady system (3) from different ball positions and to couple the paths using cross informations involving a global gradient [2, 3, 8]. Consider, q balls x_j, $j = 1, \ldots, q$, following the motion prescribed by q pseudo-unsteady systems,

$$-\dot{x_j} + \epsilon\, \ddot{x_j} = -(F_j + G_j), \tag{4}$$

where F_j is as in Eq. (3) and G_j a global gradient representing the interaction between balls (recall that each ball is a design configuration). To be able to reach the global minima, the number of balls has to be enough large. A good estimation for this number is given by the dimension of the design space (n). Even with this number the complexity is negligible compared to those of evolutionary algorithms. Our experience shows that the following choice of G_j gives satisfaction (see example below),

$$(G_j)_i = \sum_{\substack{k=1 \\ k \neq j}}^{q} \frac{J_j - J_k}{\|x_j - x_k\|^2} (x_{j_i} - x_{ki}), \qquad \text{for} \quad j = 1, \ldots, q, \quad i = 1, \ldots, n.$$

However, in CAD-free parameterization, n can be quite large and, due to the required computational effort for one simulation, we cannot afford for more than a few (say 3 or 4) shape evolutions at the same time. This approach can be seen therefore as an improvement of the search capacity of the original algorithm. In addition, the process is suitable for a distributed treatment as in evolutionary type minimizations.

We show below the behavior of the pseudo-unsteady systems (4) with two balls and constant λ and ϵ for the minimization of a function having several local minima (the global minimum is reached at (0,0)). For $(x, y) \in]-10, 10[\times]-10, 10[$ consider J defined by

$$J(x, y) = 1 - \cos(x) \cos\left(\frac{y}{\sqrt{2}}\right) + \frac{1}{50}\left(\left(x - \frac{y}{2}\right)^2 + 1.75y^2\right). \tag{5}$$

The aim is to show that heavy ball method improves global minimum search by helping to escape from local minima. Finding the global minima requires however several trials. But coupling several heavy balls can help finding the global minima using balls not converging to the global minima individually.

3. Sensitivities and incomplete sensitivities

Consider the general simulation loop, involved in (1), leading from shape parameterization or control variables to the cost function,

$$J(x) : x \to q(x) \to U(q(x)) \to J(x, q(x), U(q(x))).$$

The gradient of J with respect to x is

$$\frac{\mathrm{d}J}{\mathrm{d}x} = \frac{\partial J}{\partial x} + \frac{\partial J}{\partial q}\frac{\partial q}{\partial x} + \frac{\partial J}{\partial U}\frac{\partial U}{\partial q}\frac{\partial q}{\partial x}. \tag{6}$$

If the following requirements hold, we can introduce incomplete evaluation of this gradient, reducing its evaluation cost:

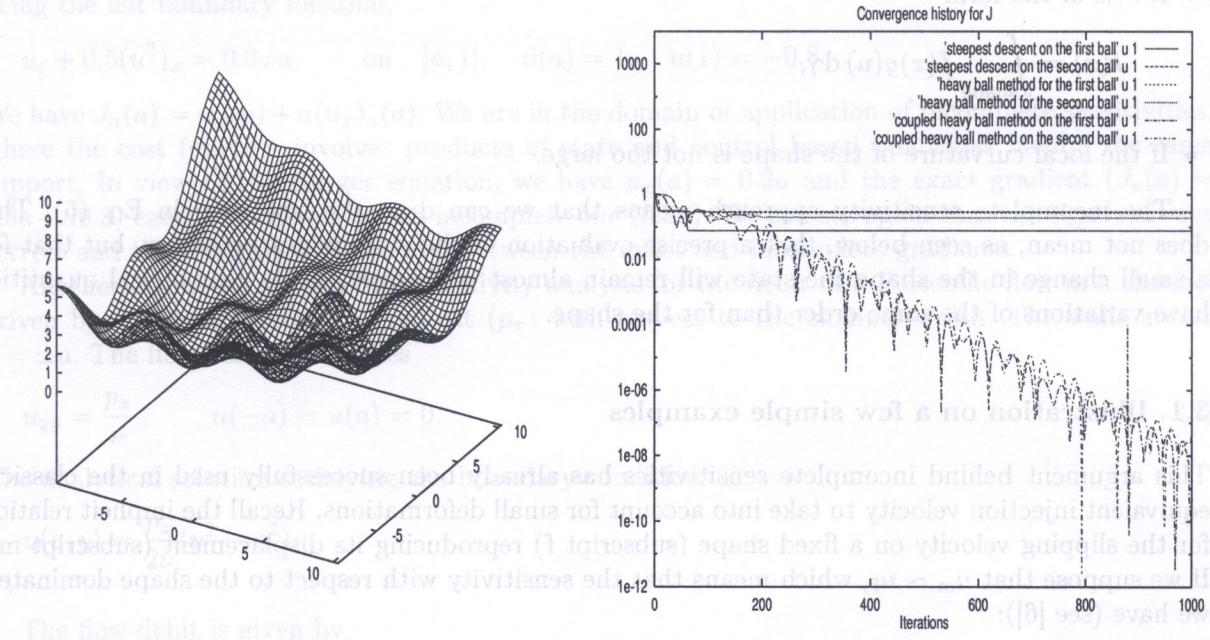

Fig. 1. Left: graph of $J(x, y)$ given by Eq. (5); right: convergence histories for the steepest descent and heavy ball methods starting from two different points, all captured by local minima

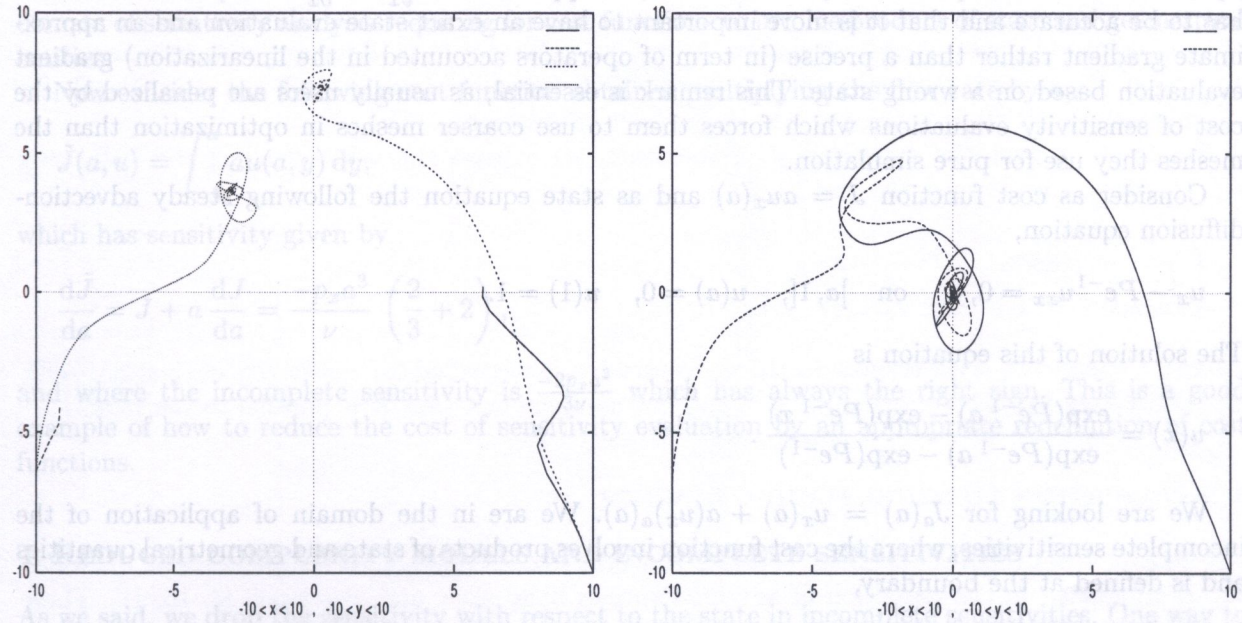

Fig. 2. Left: paths for the steepest descent and heavy ball methods starting from two different points; right: when coupling the two balls in heavy ball method using the global gradient, the global minimum is reached

- If both the cost function and control space are defined on the shape (or a same part of it),
- If J is of the form

$$J(x) = \int_{\text{shape}} f(x)g(u)\,\mathrm{d}\gamma,$$

- If the local curvature of the shape is not too large.

The incomplete sensitivity approach means that we can drop the last term in Eq. (6). This does not mean, as seen below, that a precise evaluation of the state is not necessary, but that for a small change in the shape the state will remain almost unchanged, while geometrical quantities have variations of the same order than for the shape.

3.1. Illustration on a few simple examples

This argument behind incomplete sensitivities has already been successfully used in the classical equivalent injection velocity to take into account for small deformations. Recall the implicit relation for the slipping velocity on a fixed shape (subscript f) reproducing its displacement (subscript m). If we suppose that $u_{\mathrm{m}} \sim u_{\mathrm{f}}$, which means that the sensitivity with respect to the shape dominates, we have (see [6]):

$$u_{\mathrm{f}} \cdot n_{\mathrm{f}} = -u_{\mathrm{f}}(n_{\mathrm{m}} - n_{\mathrm{f}}) + V \cdot n_{\mathrm{m}}\,, \tag{7}$$

where V is the speed of the moving shape in the fixed frame attached to the fixed shape. In the same way, sensitivity analysis for the product $u \cdot n$ with respect to the shape x gives

$$\frac{\mathrm{d}}{\mathrm{d}x}(u \cdot n) = \frac{\partial u}{\partial x} \cdot n + u\frac{\partial n}{\partial x} \sim u\frac{\partial n}{\partial x}\,,$$

where as for the transpiration condition above we supposed that $\frac{\partial u}{\partial x} \ll \frac{\partial n}{\partial x}$. We see that the state has to be accurate and that it is more important to have an exact state evaluation and an approximate gradient rather than a precise (in term of operators accounted in the linearization) gradient evaluation based on a wrong state. This remark is essential, as usually users are penalized by the cost of sensitivity evaluations which forces them to use coarser meshes in optimization than the meshes they use for pure simulation.

Consider as cost function $J = au_x(a)$ and as state equation the following steady advection-diffusion equation,

$$u_x - Pe^{-1}u_{xx} = 0, \qquad \text{on} \quad]a,1[, \quad u(a) = 0, \quad u(1) = 1.$$

The solution of this equation is

$$u(x) = \frac{\exp(Pe^{-1}\,a) - \exp(Pe^{-1}\,x)}{\exp(Pe^{-1}\,a) - \exp(Pe^{-1})}\,.$$

We are looking for $J_a(a) = u_x(a) + a(u_x)_a(a)$. We are in the domain of application of the incomplete sensitivities, where the cost function involves products of state and geometrical quantities and is defined at the boundary,

$$J_a(a) = u_x(a)\left(1 + a\,\frac{Pe^{-1}\exp(Pe^{-1}\,a)}{\exp(Pe^{-1}\,a) - \exp(Pe^{-1})}\right).$$

The second term in the parenthesis is the state linearization contribution which is negligible for large Peclet number. In all cases, the sign of the sensitivity is always correct.

The analysis also holds for nonlinear PDEs such as the Burger equation. Indeed, consider as cost function $J(a) = au_x(a)$ and as state the steady solution of the Burger equation seen before, with a being the left boundary location,

$$u_t + 0.5(u^2)_x = 0.3xu, \qquad \text{on} \quad]a, 1[, \quad u(a) = 1, \quad u(1) = -0.8.$$

We have $J_a(a) = u_x(a) + a(u_x)_a(a)$. We are in the domain of application of incomplete sensitivities, where the cost function involves products of state and control based quantities having the same support. In view of the Burger equation, we have $u_x(a) = 0.3a$ and the exact gradient ($J_a(a) = 0.3a + a0.3$) can be compared to the incomplete one ($0.3a$). We can see again that the sign is always correct and there is only a factor of 2 between the exact and incomplete gradients.

Another example concerns the sensitivity analysis for the debit of a Poiseuille flow in a channel driven by a constant pressure gradient (p_x) with respect to the channel width. The walls are at $y = \pm a$. The flow velocity satisfies

$$u_{yy} = \frac{p_x}{\nu}, \qquad u(-a) = u(a) = 0. \tag{8}$$

The analytical solution satisfying the boundary conditions is

$$u(a, y) = \frac{p_x}{2\nu}(y^2 - a^2)$$

The flow debit is given by

$$J(a) = \int_{-a}^{a} u(a, y)\,\mathrm{d}y \quad \left(= \frac{-2p_x a^3}{3\nu}\right).$$

The gradient is given by (using the boundary conditions in Eq. (8))

$$\frac{\mathrm{d}J}{\mathrm{d}a} = \int_{-a}^{a} \partial_a U(a, y)\,\mathrm{d}y = \frac{-2a^2 p_x}{\nu},$$

while the incomplete sensitivity vanishes. Indeed, in this example we are not in the validity [8] domain of sensitivity analysis requiring for cost functions to involve product of state and geometrical entities.

Now consider the following cost function obtained multiplying the flow rate by a,

$$\tilde{J}(a, u) = \int_{-a}^{a} au(a, y)\,\mathrm{d}y,$$

which has sensitivity given by

$$\frac{\mathrm{d}\tilde{J}}{\mathrm{d}a} = J + a\frac{\mathrm{d}J}{\mathrm{d}a} = \frac{-p_x a^3}{\nu}\left(\frac{2}{3} + 2\right),$$

and where the incomplete sensitivity is $\frac{-2p_x a^3}{3\nu}$ which has always the right sign. This is a good example of how to reduce the cost of sensitivity evaluation by an appropriate redefinition of cost functions.

4. Reduced complexity models and incomplete sensitivities

As we said, we drop the sensitivity with respect to the state in incomplete sensitivities. One way to cheaply improve this approximation is to use reduced models to provide these sensitivities. In other words, consider the following reduced model for the definition of $\tilde{U} \sim U$,

$$x \to q(x) \to \tilde{U}(q(x)) \begin{pmatrix} U \\ \tilde{U} \end{pmatrix},$$

where $\tilde{U}$ is the solution of a reduced low-complexity model (wall-functions for instance). The last term is an identification term for the reduced model to produce the same results that the full state equation.

The incomplete gradient of J with respect to x can be improved adding the lost part from the exact gradient, but computed based on this model,

$$\frac{\mathrm{d}J}{\mathrm{d}x} \sim \frac{\partial J(U)}{\partial x} + \frac{\partial J(U)}{\partial q}\frac{\partial q}{\partial x} + \frac{\partial J(U)}{\partial U}\frac{\partial \tilde{U}}{\partial q}\frac{\partial q}{\partial x}\frac{U}{\tilde{U}}. \tag{9}$$

We can see that, $\tilde{U}$ is never used, but only $\partial\tilde{U}/\partial q$. It is also important to notice that the reduced models need to be valid only over the support of the control parameters. We see below an example of such simplification.

5. Cost function and its redefinition

The original cost function we consider is designed to minimize the skew and band dispersion for the advected species and uses the fact that the iso-contours of an advected specie C need to remain normal to the flow velocity,

$$J(x) = \int_\omega (\nabla C \times U(\alpha))^2 \,\mathrm{d}x.$$

We see that we are not in the admissibility domain of incomplete sensitivities as the cost function is defined over the whole channel.

To be suitable for incomplete sensitivities we introduce the following approximate cost function based on migration time along the walls of the channel to minimize the skew,

$$J(x) = \left(\int_{\Gamma_i} \frac{\mathrm{d}s}{U\cdot\vec{\tau}} - \int_{\Gamma_o} \frac{\mathrm{d}s}{U\cdot\vec{\tau}}\right)^2 + \left(\int_{\Gamma_i} \left\|\frac{\partial\vec{n}}{\partial s}\right\| - \int_{\Gamma_i^0} \left\|\frac{\partial\vec{n}}{\partial s}\right\|\right)^2 + \left(\int_{\Gamma_o} \left\|\frac{\partial\vec{n}}{\partial s}\right\| - \int_{\Gamma_o^0} \left\|\frac{\partial\vec{n}}{\partial s}\right\|\right)^2,$$

where s is the curvilinear coordinate and $(\vec{\tau},\vec{n})$ a local orthonormal basis. The two last terms have been introduced to control wall regularity. Indeed, we noticed that loosing regularity increases band dispersion. We can see that the new cost function is much more complicated, but it is suitable for incomplete sensitivity reducing the cost of gradient calculation.

Finally, to reduce the dependency on the state, we express the velocity along the wall using Eq. (2). Hence, we rewrite the first term as

$$\left(\int_{\Gamma_i} \frac{-\mu\,\mathrm{d}s}{\epsilon_0\epsilon_r\zeta(\vec{\tau}\cdot\vec{E})} - \int_{\Gamma_o} \frac{-\mu\,\mathrm{d}s}{\epsilon_0\epsilon_r\zeta(\vec{\tau}\cdot\vec{E})}\right)^2,$$

where ζ dependency with respect to the concentration is neglected for sensitivity evaluation. Also, we deliberately left the dependency on $\vec{\tau}$ and not used the fact that E is parallel to the wall.

6. Application to microfluidic devices

The control and design problem we consider concerns MEMs microfluidic configurations for which we are interested in the reduction of advected species band skew and dispersion [4, 10, 11]. These systems are designed for the separation and identification of microscopic quantities present in a buffer solution submitted to an electric field. The aim is to set up the longest channel occupying the smallest surface using 180 turns. Before the band to be convected, we need to consider the problem of minimization of the dispersion of the initial extracted band. This is performed tuning the external electric field in a cross geometry. Once this band is obtained, it is convected and the

aim is to find 180 turns keeping the initial dispersion and skew unchanged. Indeed, the skew and dispersion are only due to changes in the curvature of the channel. The control parameterization is therefore based, for shape optimization, on a geometrical CAD-free model [5] and for the initial control problem on the external applied electric field. Hence, in the first case, the size n of the control space is large while it is small for the second case.

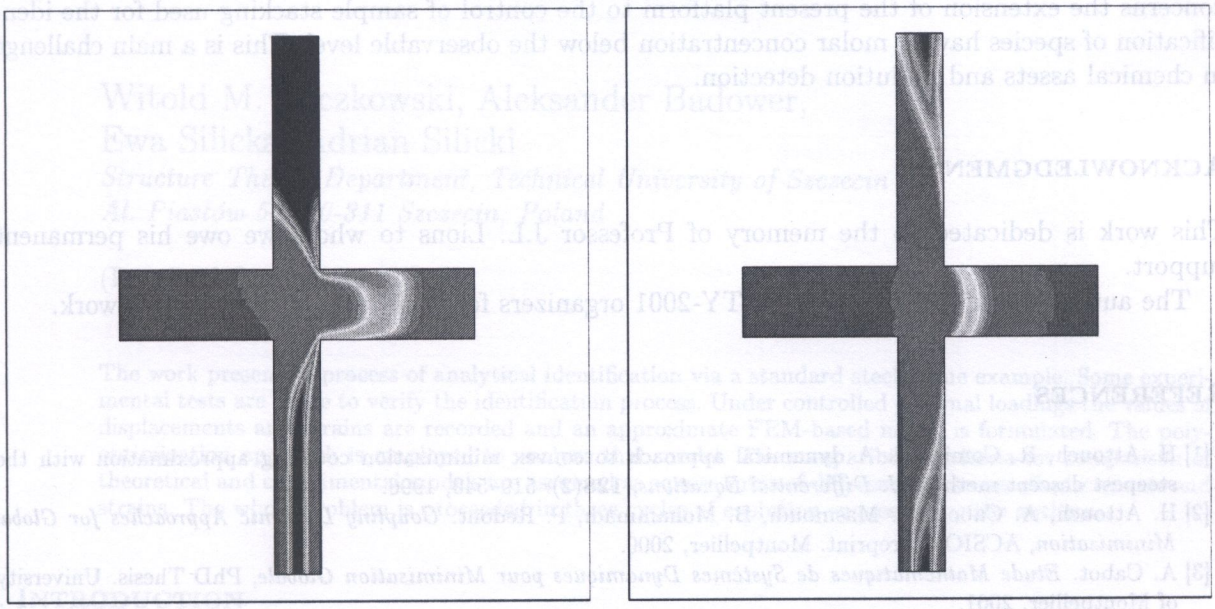

Fig. 3. Extraction algorithm – left: extracted band without controlling through the external field; right: with control the band dispersion has been reduced

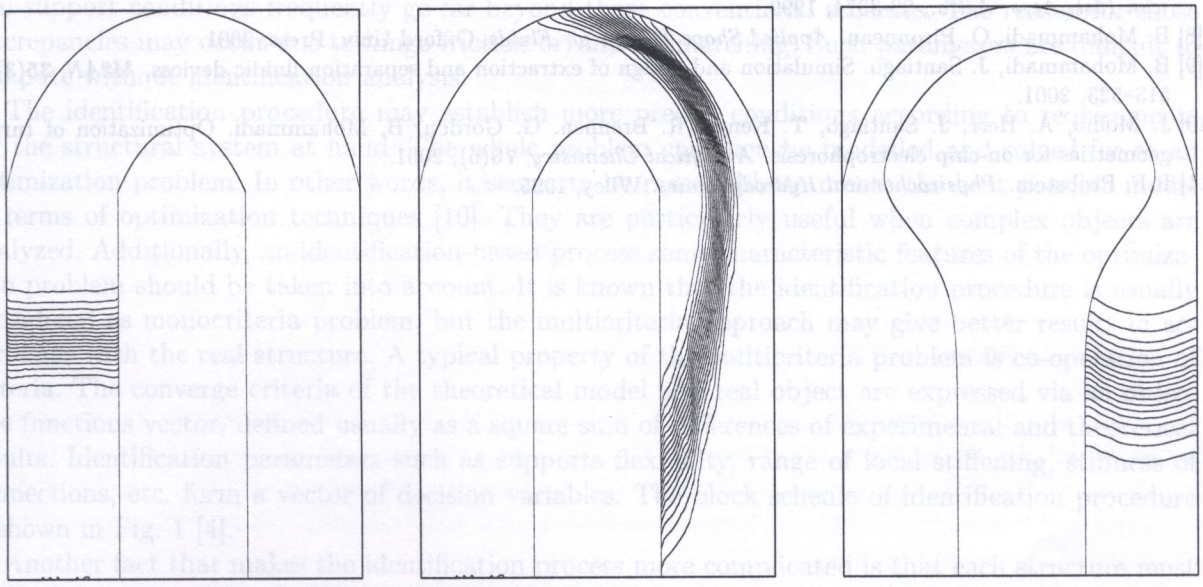

Fig. 4. Design of 180 turns minimizing the band skew – left: the original turn; right: optimized. The initial band geometry is almost conserved enabling for the separation mechanism to be the only one involved

7. Concluding remarks

The main ingredients of our minimal complexity control and optimization platform, namely incomplete sensitivity evaluation and dynamic minimization algorithms, have been presented. The minimal complexity has to be understood in the sense that design or control have the same cost that the solution of the direct problem. Applications concern the control and design of microfluidic devices to reduce advection species band dispersion and skew in microscopic channels. Current effort concerns the extension of the present platform to the control of sample stacking used for the identification of species having molar concentration below the observable level. This is a main challenge in chemical assets and pollution detection.

Acknowledgments

This work is dedicated to the memory of Professor J.L. Lions to whom we owe his permanent support.

The author would like to thank OPTY-2001 organizers for their kind interest to this work.

References

[1] H. Attouch, R. Cominetti. A dynamical approach to convex minimization coupling approximation with the steepest descent method. *J. Differential Equations*, **128**(2): 519–540, 1996.

[2] H. Attouch, A. Cabot, M. Masmoudi, B. Mohammadi, P. Redont. *Coupling Dynamic Approaches for Global Minimization*, ACSIOM preprint. Montpellier, 2000.

[3] A. Cabot. *Etude Mathématiques de Systèmes Dynamiques pour Minimisation Globale*, PhD Thesis. University of Montpellier, 2001.

[4] C.T. Culbeston, S.C. Jacobson, J. Ramsey. Dispersion sources for compact geometries on microchips, *Analytical Chemistry*, **70**: 3781–3789, 1998.

[5] B. Mohammadi. *Practical Applications to Fluid Flows of Automatic Differentiation for Design Problems.* VKI lecture series, 1997-05, 1997.

[6] B. Mohammadi. Flow control and shape optimization in aeroelastic configurations. *American Inst. Aero. Astro.*, 99-0182, 1999.

[7] B. Mohammadi. Dynamical approaches and incomplete gradients for shape optimization and flow control. *American Inst. Aero. Astro.*, 99-3374, 1999.

[8] B. Mohammadi, O. Pironneau. *Applied Shape Design for Fluids.* Oxford Univ. Press, 2001.

[9] B. Mohammadi, J. Santiago. Simulation and design of extraction and separation fluidic devices, *M2AN*, **35**(3): 513–523, 2001.

[10] J. Molho, A. Herr, J. Santiago, T. Kenny, R. Brennen, G. Gordon, B. Mohammadi. Optimization of turn geometries for on-chip electrophoresis. *Analytical Chemistry*, **73**(6), 2001.

[11] R.F. Probstein. *Physicochemical Hydrodynamics.* Wiley, 1995.